Quasi-free proton knockout from 12C on carbon target at 398 MeV/u

Physics Letters B 797 (2019) 134802

Contents lists available at ScienceDirect

Physics Letters B

www.elsevier.com/locate/physletb

Quasi-free proton knockout from ^{12}C on carbon target at 398 MeV/u

V. Panin [a,*], M. Holl [a], J.T. Taylor [b], Y. Aksyutina [c], H. Alvarez-Pol [d], T. Aumann [a,c], C.A. Bertulani [e], K. Boretzky [c], C. Caesar [a], M. Chartier [b], L.V. Chulkov [f], D. Cortina-Gil [d], J. Enders [a], O. Ershova [g], H. Geissel [c], R. Gernhäuser [h], M. Heil [c], H.T. Johansson [i], B. Jonson [i], A. Kelić-Heil [c], O. Kiselev [c], C. Langer [g], T. Le Bleis [h], R. Lemmon [j], T. Nilsson [i], S. Paschalis [a], M. Petri [a], R. Plag [c], R. Reifarth [g], D. Rossi [c], H. Scheit [a], H. Simon [c], F. Wamers [a,c], H. Weick [c], C. Wimmer [g]

[a] Institut für Kernphysik, Technische Universität Darmstadt, 64289 Darmstadt, Germany
[b] Oliver Lodge Laboratory, University of Liverpool, Liverpool L69 7ZE, United Kingdom
[c] GSI Helmholtzzentrum für Schwerionenforschung, 64291 Darmstadt, Germany
[d] IGFAE, Instituto Galego de Física de Altas Enerxías, Universidade de Santiago de Compostela, E-15782 Santiago de Compostela, Spain
[e] Department of Physics and Astronomy, Texas A&M University-Commerce, Commerce, TX 75429, USA
[f] NRC Kurchatov Institute, Ru-123182 Moscow, Russia
[g] Goethe-Universität Frankfurt am Main, 60438 Frankfurt am Main, Germany
[h] Physik Department E12, Technische Universität München, 85748 Garching, Germany
[i] Department of Physics, Chalmers Tekniska Högskola, S-412 96 Göteborg, Sweden
[j] STFC Daresbury Laboratory, Daresbury, Warrington WA4 4AD, United Kingdom

ARTICLE INFO

Article history:
Received 8 February 2019
Received in revised form 19 July 2019
Accepted 19 July 2019
Available online 24 July 2019
Editor: D.F. Geesaman

Keywords:
Direct nuclear reactions
One-nucleon removal
Quasi-free scattering
Cross sections

ABSTRACT

The proton-removal mechanism of the $^{12}C \rightarrow ^{11}B$ reaction induced on a carbon target via elementary nucleon-nucleon scattering is investigated in exclusive triple-coincidence measurements. The observed two-nucleon angular correlations are found to be consistent with quasi-free scattering of a projectile-like proton off a target-like nucleon. Exclusive cross sections for one-step *pp* and *pn* interactions are determined as σ_{pp}=17.2(12) mb and σ_{pn}=18.2(18), respectively. The extracted quasi-free component amounts up to 58(4)% of the total proton-removal cross section. The results are compared to total proton-removal cross sections obtained from the experiment and eikonal reaction theory.

At relativistic beam energies up to a few GeV per nucleon, the nucleus-nucleus fragmentation process can proceed through direct removal of one or several constituent nucleons. The most common experimental approach to study one-nucleon removal is based on an inclusive measurement of the (A-1) residue of an energetic projectile A, after impinging on a light target nucleus such as carbon or beryllium. Due to the relatively simple experimental scheme and applicability of certain theoretical approximations [1–3], this method is ubiquitously used to quantify the single-particle character of the nuclear wave function of isospin-asymmetric nuclei [4]. On the other hand, an accurate formulation of the inclusive reaction dynamics of many-body systems is intricate due to the interplay of multiple degrees of freedom, involving direct knockout, soft nuclear excitations, Coulomb breakup, final-state interactions, absorption effects etc. [1,5–7].

Different types of inclusive experiments have studied protons and other light particles emerging from ion-ion collisions at various energies [8–12]. The results were discussed in the context of formation of a hot quasi-equilibrated nuclear fireball [8], nucleon-nucleon (NN) scattering [13] and intra-nuclear cascades [14] etc., showing that one or another reaction mechanism is probed under certain kinematical conditions and for certain nuclear masses. Observation of multiple outgoing particles and their correlations has allowed to draw a more accurate picture of the collision process. In particular, it was found that outgoing pairs of protons, emerging at large transverse momenta relative to the beam, can be qualitatively explained by one-step elastic scattering of a proton bound in the projectile with a proton bound in the target nucleus, (at least

* Corresponding author.
E-mail addresses: valerii.panin@riken.jp, valerii.panin@cea.fr (V. Panin).

https://doi.org/10.1016/j.physletb.2019.134802

for light nuclear systems) as a result of peripheral grazing of the two nuclei [15]. In this case, azimuthal *pp* correlations were suggested to give a definitive indication of the elementary scattering process [16].

Other studies, in which the (A-1) fragment and a removed nucleon were observed in coincidence, demonstrated the validity of the sudden and eikonal approximations [17]. It was shown that the reaction can be described by two main interaction terms: nucleon removal through elementary NN scattering, involving large momentum transfer (knockout), or through evaporation after exciting the projectile above the particle threshold (inelastic scattering). Although one-nucleon removal encompasses any process producing an (A-1) nucleus in the final state, the two mechanisms mentioned above can be clearly separated in the reaction theory as well as experimentally due to the rather different kinematics of the escaping nucleon(s). In the latter case, the nucleon(s) has (have) a velocity close to the projectile velocity and small ($<$ 100 mrad) angles relative to the beam, while a broad angular distribution around 45° is expected for the knockout process as also shown by the data discussed later. Still, the total one-nucleon removal process is sometimes referred to in the literature as (heavy-ion induced) knockout. Furthermore, the two contributing processes are often called "stripping" and "diffraction". Such terminology appears to be confusing as stripping is commonly used for transfer reactions and diffraction or elastic breakup may generally be associated with projectile excitation through scattering including collective excitations (inelastic in such case). These ambiguities are best resolved under detailed microscopic view on the nucleon removal mechanism, which can be investigated in the most exclusive measurements and which is, therefore, crucial to establish a reliable reaction formalism.

In the eikonal approach [6,7,4,18], which is widely used to describe the nucleon removal in a broad range of energies and nuclear masses, including isospin-asymmetric nuclei [19,20], the total cross section $A\rightarrow(A\text{-}1)$ can be written as the sum:

$$\sigma_{\rm tot} = \sigma_{\rm ko} + \sigma_{\rm inel}, \tag{1}$$

where $\sigma_{\rm ko}$ is the knockout cross section related to the interaction of the removed nucleon with the target nucleons, and $\sigma_{\rm inel}$ is the cross section for nuclear inelastic scattering when the projectile decays to the (A-1) fragment (Coulomb dissociation is a part of this cross section but can be neglected for light targets). In most cases $\sigma_{\rm ko}$ is the dominant channel involving NN interaction of the struck nucleon with the target, in particular through quasi-free scattering (QFS) of the removed nucleon off a nucleon bound in the target, when no further interaction occurs and both particles escape the reaction zone as schematically depicted in Fig. 1. Thus, $\sigma_{\rm ko}$ can be represented as the sum:

$$\sigma_{\rm ko} = \sigma_{\rm QFS} + \sigma_{\rm res}, \tag{2}$$

where $\sigma_{\rm QFS}$ is the quasi-free knockout cross section and $\sigma_{\rm res}$ contains all other reaction channels, including QFS followed by secondary interactions with the nuclear environment, when the (A-1) fragment survives but at least one of the scattered particles is "absorbed" from the QFS channel. For the proton knockout $^{12}\text{C}\rightarrow{}^{11}\text{B}$, discussed in this paper, we consider the two cases of proton-proton (pp) and proton-neutron (pn) QFS processes.

In a very simple model, a quasi-free knockout reaction between two nuclei with 4-momenta P and Q can be described as scattering of two internal nucleons with initial off-shell 4-momenta p_1 and q_1 to the final on-shell states p_2 and q_2. The reaction kinematics is restricted by the conservation of momentum and energy at each vertex (1, 2 and 3 in Fig. 1). At the energy regime of the present experiment, the *pp* scattering in the center-of-mass (CM) is taken to be approximately isotropic, while for the *pn* case a realistic CM angular anisotropy is introduced through the parameterization of the free *pn* differential cross section calculated in the PWA-framework [21]. Internal 3-momenta associated with p_1 and q_1 are both approximated by the measured recoil momentum distribution of ^{11}B in the rest-frame of the ^{12}C projectile (Fig. 4). One assumes the experimental scheme in which two outgoing nucleons are detected in triple coincidence with the projectile-like spectator ^{11}B, but the target-like spectator (^{11}B or ^{11}C) remains unobserved due to small kinetic energy. Despite its simplicity, the model is found to be in remarkable agreement with the experiment as shown in Fig. 3 and explained in the following sections. A Monte-Carlo event generator utilizing this reaction model was implemented into the Geant4-based R3BRoot simulations [22,23] in order to evaluate the experimental response of the setup.

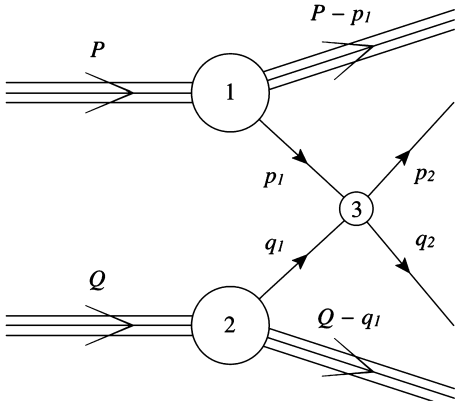

Fig. 1. Diagrammatic representation of the nucleus-nucleus collision proceeding through one-step QFS scattering of two nucleons with 4-momenta p_1 and q_1, bound in the projectile nucleus and in the target nucleus with 4-momenta P and Q, respectively.

Experiment and results. The experimental setup was identical to the one reported in [24]. A primary ^{12}C beam at an energy of 400 MeV/u was directed onto a 370(7) mg/cm^2 carbon target. The beam energy in the middle of the target was ≈398 MeV/u. Outgoing particles, emerging at large angles ($>$ 7.5°) relative to the beam, were measured using a combination of the 4π-calorimeter Crystal Ball (CB) and an array of silicon-strip detectors (SSDs) surrounding the target. Reaction fragments, emitted in the beam direction, were identified via magnetic-rigidity, time-of-flight and energy-loss analysis after the large dipole magnet ALADIN, which allowed for an event-by-event measurement of outgoing ^{11}B residues (see Fig. 2). In addition, empty-target (ET) measurements were performed to account for background reactions in the beam-line detectors. Two-particle events in coincidence with ^{11}B residues were identified by counting the number of high-energy clusters of crystals ($N_{\rm C}$) in the forward hemisphere of the CB. For this purpose, an add-back procedure was carried out for the CB data and all events with $N_{\rm C}$=2 were selected under the condition to have at least one crystal with an energy above 25 MeV in each cluster. The angular information from the CB clusters was used either separately, with somewhat poor resolution but large angular coverage, or in combination with coincident hits in the SSDs, which provided good angular resolution but smaller angular acceptance (between 14° and 64° in polar direction relative to the beam). The resulting angular resolution in the CB is around 10° (sigma) compared to 1°-2° in the SSDs. In both cases, spherical angles of two outgoing particles can be redundantly reconstructed

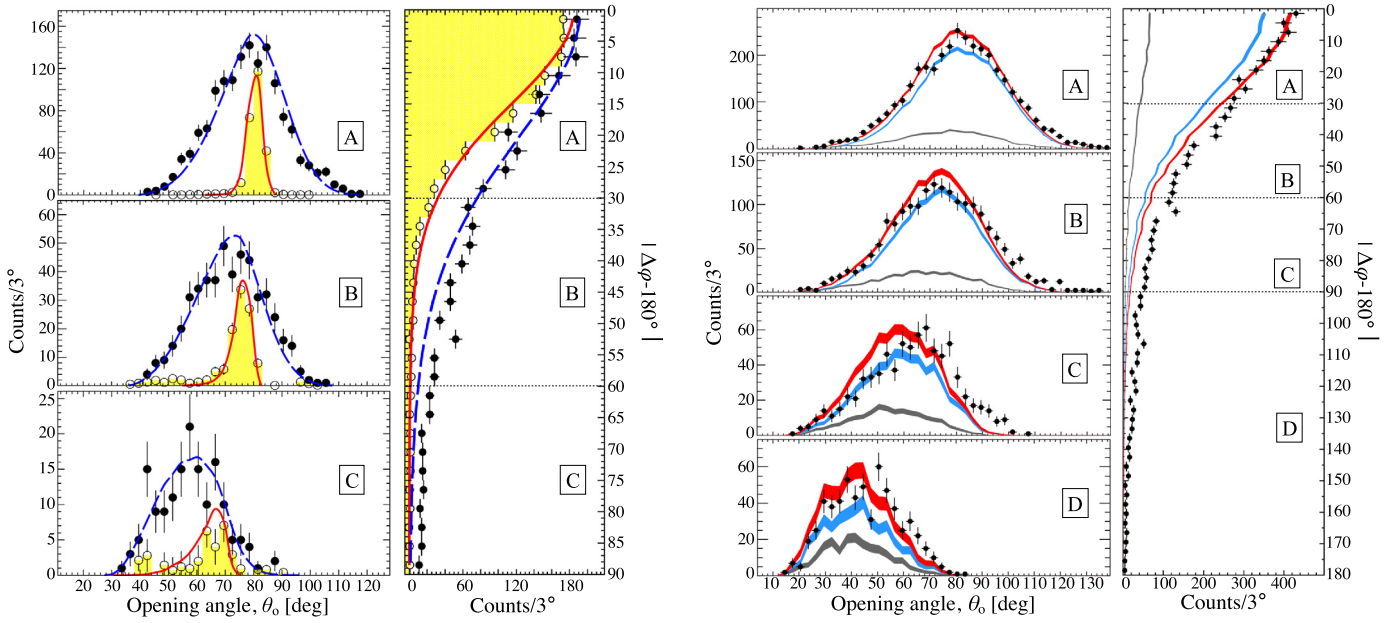

(a) Angular correlations from SSDs

(b) Angular correlations from CB

Fig. 3. Two-particle angular correlations in coincidence with outgoing ^{11}B. Empty target contribution is subtracted from the data. Fig. (a) displays experimental distributions of *pp* pairs (black circles with error bars) measured by the SSD array. For comparison, (a) shows arbitrarily scaled *pp* correlations from the ^{12}C$(p, 2p)^{11}$B reaction on a hydrogen target (empty circles, yellow-filled area), which were measured with the same setup [24]. Left panel of (a) shows the opening angle θ_o of two outgoing protons for different intervals of $|\Delta\varphi - 180°|$: A=[0°, 30°], B=[30°, 60°] and C=[60°, 90°], as indicated on the right panel of (a). Solid red lines and dashed blue lines in (a) are the corresponding kinematical curves, which take into account angular resolution and acceptance of the SSDs. Similarly, (b) shows experimental distributions (black circles with error bars) using the angular information only from the CB, regardless of coincidences in SSDs and with an additional interval "D" corresponding to $90° < |\Delta\varphi - 180°| < 180°$. Blue, grey, and red lines in (b) are fitted results of the R3BRoot simulations for *pp*, *pn* reactions and their sum, respectively, with line thickness corresponding to the statistical uncertainties. Scaling parameters for fitting each reaction channel are obtained from the CB multiplicity analysis (see Fig. 6) and are adjusted to fit the sum of *pp* and *pn* contributions to the experimental data in the interval "A" in the right panel of (b). After that, the extracted ratios of *pp* and *pn* reactions from every interval (A, B, C and D) are fitted to the corresponding θ_o distributions in the left panel of (b).

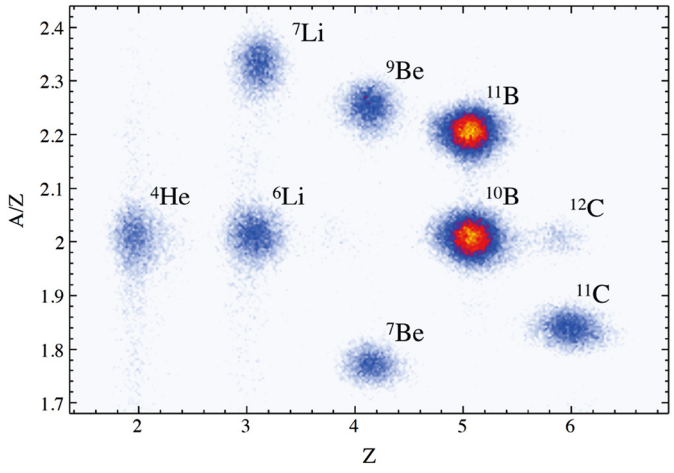

Fig. 2. Mass-over-charge (A/Z) and charge (Z) identification of outgoing beam-like fragments in coincidence with high-energy signal in the Crystal Ball.

in polar $(\vartheta_1, \vartheta_2)$ and azimuthal (φ_1, φ_2) directions relative to the beam. Two-particle correlations are then investigated through their azimuthal relation:

$$|\varphi_1 - \varphi_2 - 180°| \equiv |\Delta\varphi - 180°|, \tag{3}$$

which is called "coplanar angle", and through the "opening" (relative) angle θ_o between the particles given by:

$$\cos\theta_o = \sin\vartheta_1 \sin\vartheta_2 \cos(\varphi_2 - \varphi_1) + \cos\vartheta_1 \cos\vartheta_2. \tag{4}$$

In Fig. 3, the measured distributions of these two angles in coincidence with outgoing ^{11}B are compared to the simulated distributions for *pp* and *pn* QFS reactions. The simulations are based on the above described reaction formalism and are analyzed using an identical procedure as applied to the experimental data.

The QFS origin of the outgoing particles is reflected in a dominant yield of coplanar reactions at $|\Delta\varphi - 180°| \approx 0°$, a broad peak in the θ_o distribution and in the characteristic dependence of θ_o on the coplanar-angle cut. The apparent shift of the θ_o peak with increasing $|\Delta\varphi - 180°|$ is due to off-plane reactions being more sensitive to large transverse components of the initial total 3-momentum $\boldsymbol{p_1} + \boldsymbol{q_1}$ of the nucleon pair (Fig. 1). The Fermi motion of the target nucleon manifests in a larger width of θ_o distribution as compared to the QFS reaction ^{12}C$(p, 2p)^{11}$B on a hydrogen target (Fig. 3a), where the target nucleon is at rest. It is important to note that due to strong absorption effects the reactions are limited to more peripheral collisions in comparison with QFS reactions on hydrogen, which allow for a much broader range of impact parameters. A quantitative comparison of impact parameters in proton removal on hydrogen and carbon targets can be found in Fig. 9 of Ref. [18].

In all simulations the Fermi momenta of both interacting nucleons were assumed to be equivalent to the measured recoil momentum of the outgoing ^{11}B (Fig. 4), which can be reasonably well described by the quasi-free knockout of a proton from the *p*-shell in ^{12}C [24]. Owing to the isospin symmetry of ^{12}C, the Fermi momenta of protons and neutrons are expected to yield very similar distributions. This is reflected in the similarity of correlation patterns reconstructed in SSDs, which are sensitive to *pp* reactions, and in CB, which is sensitive to both *pp* and *pn* events (Fig. 3b). In both cases, the widths of the angular distributions are dominated

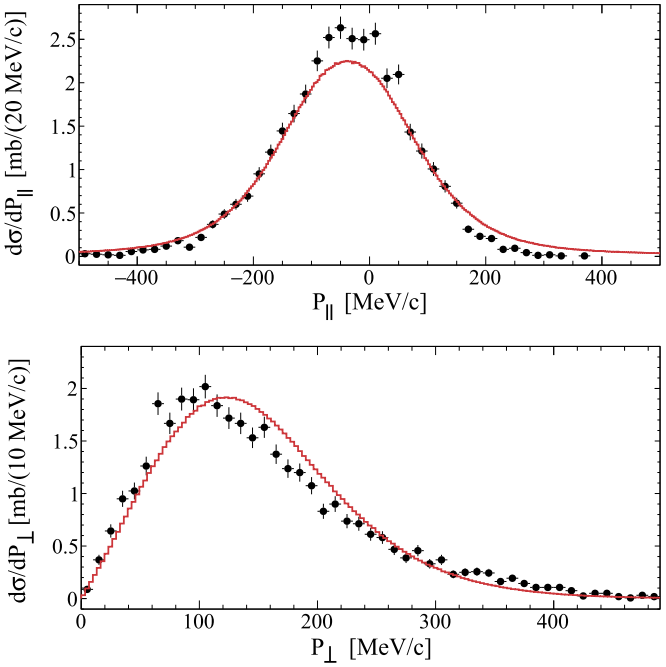

Fig. 4. Measured parallel (top) and transverse (bottom) recoil momentum distributions of ^{11}B in the rest frame of ^{12}C. The experimental data points are shown as black circles. Red lines represent the scaled theoretical calculations for ^{12}C$(p,2p)^{11}$B reaction on hydrogen target obtained in the previous work [24] and folded with the present experimental resolutions. The theoretical distribution for $P_{\parallel}$ is additionally shifted by −37 MeV/c to fit the experimental mean value.

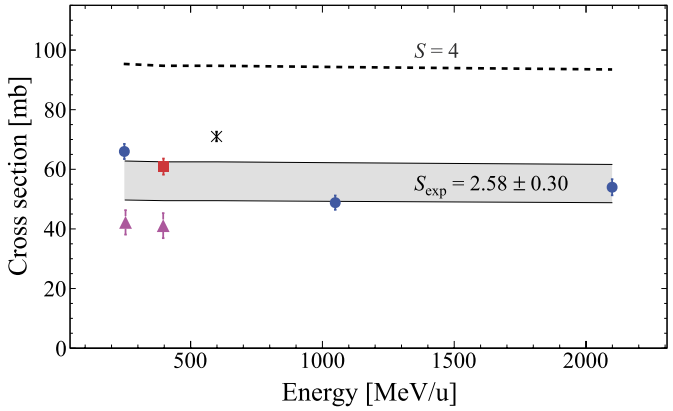

Fig. 5. Inclusive proton-removal ^{12}C→^{11}B cross sections on carbon target. The value oft 60.9(27) mb obtained in this experiment is shown as a red square at 398 MeV/u beam energy. The results from other experiments at different beam energies are shown as: blue circles (Kidd et al. [25]), black cross (Webber et al. [26]) and magenta triangles (Ogawa et al. [27]). In addition, the eikonal theory cross section for the removal of p-shell nucleon with the spectroscopic factor S=4 is shown by a dashed line. The grey shaded area shows the same theoretical result for $S_{\rm exp}$=2.58(30), extracted from the previous work [24], with the upper and lower borders representing the error of $S_{\rm exp}$.

by the reaction kinematics due to the nuclear Fermi motion. It can be noted that the observed reactions are slightly less coplanar than expected from the theory. Such deviation can be attributed to unaccounted large-momentum components of the target nucleons, because only p-shell nucleons from both, projectile and the target, were assumed in the simulations. Since the target residue is not observed in the experiment, knockout from the deeply bound s-shell or from short-range correlated pairs may also contribute. In Fig. 3, the experimental results are compared to simulated responses only from pp and pn QFS channels, both yielding similar distributions. Other possible QFS channels at any target-like cluster heavier than proton or neutron (e.g. ^{2}H, ^{3}H, ^{4}He, etc.), are estimated to produce rather different angular distributions, which fall largely outside the experimental cuts and can therefore be neglected in the present analysis.

The cross section analysis proceeded through identification and counting of incoming ^{12}C and outgoing ^{11}B nuclei (see Fig. 2). Empty target measurements were used to remove contributions of background reactions in the materials of the beamline detectors. The method to extract the cross sections is similar to the one explained in [24]. The total inclusive cross section $\sigma_{\rm tot}$=60.9(27) mb was obtained for the p-removal reaction ^{12}C→^{11}B on the carbon target. In Fig. 5 this value is compared to the data from the literature [25–27] and to the theoretical eikonal calculations similar to the ones described in [28]. Assuming the spectroscopic factor S=4 for l=1 nucleons in the independent-particle model of ^{12}C, the theoretical single-particle cross section is scaled using the method described in [28] (dashed line in Fig. 5). In addition, the same single-particle cross section is shown with the scaling parameter corresponding to the spectroscopic factor $S_{\rm exp}$=2.58(30), which was extracted in the previous work [24]. The present inclusive cross section agrees well with other experiments as well as with the theoretical expectations.

In the following analysis, the same data set of preselected ^{11}B events is used with an additional condition to observe two high-energy clusters ($N_{\rm C}$=2) in the CB. Identification of the outgoing ^{11}B allows to assign one CB cluster to a proton removed from the projectile, while the type of the second particle is ambiguous because the target residue is not observed. Since both channels, pp and pn, can contribute, as concluded from the angular correlation analysis, the observed events are fully attributed only to these two types of reactions. In order to extract their relative contributions to $N_{\rm C}$=2 events, the experimental response of CB is compared to the one extracted from the R3BRoot simulations for pp and pn reaction channels.

The most indicative parameter to distinguish between pp and pn events in the CB is the integrated crystal multiplicity M in two high-energy clusters. The total energy deposition in the CB cannot be used for this purpose because of the poor calorimetric properties of CB crystals for high-energy neutrons and protons. Due to strong electromagnetic stopping, protons deposit energy predominantly in a single crystal, while neutrons, involving hadronic interactions, can generate showers of particles which induce larger average M per event. This is illustrated in Fig. 6 where the experimental M distribution for $N_{\rm C}$=2 events (ET subtracted) is compared to the R3BRoot simulations. For the pp channel, the M distribution peaks at M=2, and for pn events it is centered around M=4. By fitting the simulated M distributions to the experimental data, as shown in Fig. 6, the relative yields of pp and pn reactions for $N_{\rm C}$=2 events are extracted as Y_{pp}=82.2(17)% and Y_{pn}=17.8(13)%, respectively, with the errors representing the fit quality. The $N_{\rm C}$=2 detection efficiencies for pp and pn channels are also determined from the R3BRoot simulations as ϵ_{pp}=61.0% and ϵ_{pn}=12.5%, respectively. Taking R_2 to be the total number of $N_{\rm C}$=2 events, one can evaluate the true numbers of pp and pn reactions (R_{pp} and R_{pn}) as following:

$$R_{pp} = R_2 Y_{pp}/\epsilon_{pp}, \tag{5}$$

$$R_{pn} = R_2 Y_{pn}/\epsilon_{pn}. \tag{6}$$

The resulting QFS cross sections associated with pp and pn interactions are $\sigma_{pp} = 17.2(12)$ mb and $\sigma_{pn} = 18.2(18)$ mb with the errors combining both, statistical and systematical uncertainties.

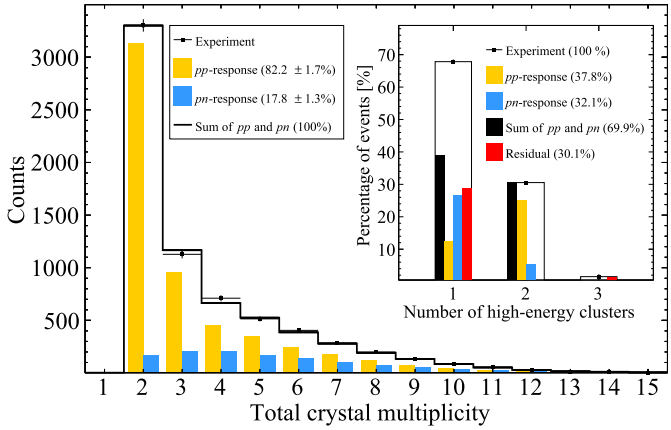

Fig. 6. Summed multiplicity M of crystals in two high-energy clusters observed in coincidence with outgoing ^{11}B fragments. Black circles with error bars represent the experimental data for N_C=2. Fitted contributions from the pp and pn reactions are indicated by the yellow and blue bars, respectively, and their sum is shown by a black solid line. The legend of the histogram shows the fit results (relative contributions) with the corresponding errors of the fit. The inset figure displays the N_C distribution for the events with $N_C>0$. The relative contribution of the pp and pn events and their sum, as extracted from the analysis of N_C=2 events, is shown with the same color code and explained by the legend of the inset figure (see text for details). In addition, the result of subtraction of the pn and pp contributions from the $N_C>0$ data is shown by red color ("Residual").

Table 1
Experimental and theoretical cross sections for the p-removal cross section $^{12}C\rightarrow{}^{11}B$ on a carbon target. The values in square brackets show percentage of the relative contribution with respect to the total cross sections shown in the bottom row of the table.

This experiment				Theory[a]	
σ_{pp}, mb	σ_{pn}, mb	$\sigma_{\rm inel}$, mb	$\sigma_{\rm res}$, mb	$\sigma_{\rm inel}$, mb	$\sigma_{\rm ko}$, mb
17.2(12) [28%]	18.2(18) [30%]	2.6(5) [4%]	22.9(35) [38%]	6.7(8) [12%]	49.3(57) [88%]
Sum: 35.4(22) [58%]		Sum: 25.5(35) [42%]			
Total: 60.9(27) mb [100%]				Total: 56.0(65) mb [100%]	

[a] Using the spectroscopic factor $S_{\rm exp}=2.58(30)$ extracted in the previous work [24].

The obtained ratio $\sigma_{pn}/\sigma_{pp}\approx 1.06(18)$ is close to the ratio 1.27 for free pp and pn cross sections at around 400 MeV, which is consistent with the QFS interpretation of the reaction mechanism in the isospin symmetric ^{12}C-^{12}C system.

The part of the p-removal cross section $\sigma_{\rm inel}$ stemming from inelastic excitation, was extracted from the analysis of ^{11}B events with N_C=0 and in coincidence with a beam-like proton in the proton-detection arm. Protons were measured by the two drift chambers and by the dedicated plastic time-of-flight wall after the ALADIN magnet. The method was similar to the one described in [29]. A tracking efficiency of 49(3)% in the proton-arm detectors was extracted from coincidences with proton hits in the in-beam SSDs directly after the target. Hence, the inelastic p-removal cross section is determined as $\sigma_{\rm inel}$=2.6(5) mb or about 4% of the total inclusive cross section $\sigma_{\rm tot}$. Direct subtraction yields $\sigma_{\rm ko}$=58.3(27) mb for the knockout mechanism of the proton removal (Eq. (1)). Thus, the summed contribution of pp and pn QFS channels amounts to 35.4(22) mb or approximately 61(5)% of $\sigma_{\rm ko}$.

Additional information is obtained from the analysis of all ^{11}B events with $N_C>0$, which accumulate about 74% of the experimental statistics for ^{11}B. The experimental N_C distribution after subtraction of ET data is shown in the inset histogram of Fig. 6. In addition, simulated N_C distributions are shown corresponding to pp and pn events, which are scaled to fit their sum at N_C=2 bin in the proportion extracted from the analysis of the N_C=2 data. The remaining part of $N_C>0$ events, which cannot be assigned to pp and pn knockout, is dominated by N_C=1 and accounts for about 30% of all $N_C>0$ events. In the present analysis it is not possible to conclude which particles contribute to N_C=1 events. They can be interpreted as a result of either background from unresolved competing QFS channels or as absorption of one outgoing QFS nucleon in the target nucleus. Another possibility due to nucleon-transfer type of reactions can be ruled out by theoretical estimation using a well-established DWBA code [30]. For example, the cross section ^{12}C(^{12}C,^{11}C)^{13}C for the transfer between the $p_{3/2}$ to $p_{1/2}$ neutron orbitals is expected to decrease quickly as the projectile energy increases, i.e. from 0.103 mb at 10 MeV/u to 2.06×10^{-3} mb at 100 MeV/u. At 400 MeV/nucleon the cross section drops to 2.33×10^{-9} mb and to even smaller value for ^{12}C(^{12}C,^{11}B)^{13}N. Another estimate using the FRESCO code [31] yielded $\sim10^{-7}$ mb for it. Although some evidence of the transfer processes was found in nucleon-removal reactions slightly below 100 MeV/u [17], their contribution to the total cross section was on the order of 10% so that one may expect practically negligible values at our beam energy. An alternative reaction channel due to excitation of sub-nucleonic degrees of freedom (e.g. Δ resonance) can be also considered, as shown by the recent studies [32]. However, the contribution of such process in the reaction cross section is estimated to be on the maximum level of only 3% as follows from direct comparison of the total and inelastic NN cross sections at around 400 MeV [33]. Hence, we refer $\sigma_{\rm res}$ as a residual part of the total cross section, which is not exhausted by one-step pp or pn QFS channels and by inelastic excitation channels, and which includes a significant fraction of the N_C=1 events.

The results of the cross section analysis are summarized in Table 1. For comparison, theoretical calculations based on the eikonal reaction theory are shown in the same table assuming a spectroscopic factor $S_{\rm exp}=2.58(30)$ for p-shell protons, which was determined in the previous work [24]. Good agreement is found between the theoretical and experimental inclusive p-removal cross

sections. The sum of σ_{pp} and σ_{pn} accounts for about 58% of the total p-removal cross section, and the remaining part is almost completely attributed to $\sigma_{\rm res}$ which can be related predominantly with the exceeding N_c=1 events in the CB. Taking into account small nucleon transfer cross sections, one possible interpretation of this result is that an outgoing nucleon after quasi-free scattering is "lost" due to absorption in the target nucleus while the second nucleon freely escapes the interaction zone. Such a two-step mechanism is not taken into account in eikonal theories used to analyze nucleon-removal reactions, and it can result in additional reduction of the survival probability for (A-1) fragments. Since this effect is expected to be larger for well-bound nucleons compared to loosely bound nucleons (because of the different extension of single-particle densities), it could possibly give a sizeable contribution to the reduction of cross sections for knockout of more deeply bound nucleons as found in intermediate-energy nucleon-removal reactions compared to theoretical cross sections [19]. This reduction of the cross section is so far not explained and is not seen in quasi-free knockout reactions in comparison with the theoretical predictions [20]. In the latter case, absorption of nucleons after QFS due to subsequent binary collisions are explicitly taken into account in the theory [18].

Summary. Triple-coincidence measurements of the p-removal reaction $^{12}C\rightarrow^{11}B$ on a carbon target at 398 MeV/u demonstrate that elementary quasi-free nucleon-nucleon scattering accounts for more than half of the total removal cross section. This is reflected in the angular distributions of the outgoing nucleon pairs, which exhibit characteristic correlation patterns and can be explained by a rather simple QFS reaction model. QFS reactions due to pp and pn interactions are separately quantified and estimated to contribute nearly equally to the knockout cross section, as can be also expected from the similarity of free pn and pp cross sections at this energy, and from the proton-neutron symmetry of the interacting nuclear systems. The momentum distributions and angular correlations can be well described assuming a QFS process if the Fermi motion of target nucleons is taken into account. Events with only one high-energy particle measured at large angles in coincidence with ^{11}B exhaust a surprisingly large fraction of the knockout part of the total cross section. However, from the present analysis it is difficult to conclude on the type and origin of such events so that they are fully attributed to the residual cross section along with other possible unresolved channels leading to proton removal from ^{12}C projectile. Theoretical estimations of negligibly small nucleon-transfer cross sections allow to speculate on the possible origin of these events as being due to secondary reaction (absorption) of one outgoing QFS nucleon in the target nucleus. This can potentially influence the interpretation of the reduction of the cross sections extracted from other knockout experiments.

Acknowledgements

The authors acknowledge support from HIC for FAIR, the GSI-TU Darmstadt cooperation agreement, the BMBF under Contract No. 05P19RDFN1, the Helmholtz Alliance EMMI, the Swedish Research Council, the U.S. NS Grant No. 1415656, the DOE grant No. DE-FG02-08ER41533 and the Spanish research agency MINECO under Project No. FPA2015-69640-C2-1-P.

References

[1] C.A. Bertulani, K.W. McVoy, Phys. Rev. C 46 (1992) 2638, https://doi.org/10.1103/PhysRevC.46.2638.
[2] J. Hüfner, M.C. Nemes, Phys. Rev. C 23 (1981) 2538, https://doi.org/10.1103/PhysRevC.23.2538.
[3] K. Hencken, G. Bertsch, H. Esbensen, Phys. Rev. C 54 (1996) 3043–3050, https://doi.org/10.1103/PhysRevC.54.3043.
[4] J.A. Tostevin, A. Gade, Phys. Rev. C 90 (2014) 057602, https://doi.org/10.1103/PhysRevC.90.057602, arXiv:1409.6576.
[5] M.S. Hussein, K.W. McVoy, Nucl. Phys. A 445 (1985) 124–139, https://doi.org/10.1016/0375-9474(85)90364-1.
[6] C.A. Bertulani, A. Gade, Comput. Phys. Commun. 175 (2006) 372–380, https://doi.org/10.1016/j.cpc.2006.04.006, arXiv:nucl-th/0602048.
[7] P.G. Hansen, J.A. Tostevin, Annu. Rev. Nucl. Part. Sci. 53 (2003) 219, https://doi.org/10.1146/annurev.nucl.53.041002.110406.
[8] G.D. Westfall, et al., Phys. Rev. Lett. 37 (1976) 1202–1205, https://doi.org/10.1103/PhysRevLett.37.1202.
[9] W.G. Lynch, L.W. Richardson, M.B. Tsang, R.E. Ellis, C.K. Gelbke, R.E. Warner, Phys. Lett. B 108 (1982) 274–278, https://doi.org/10.1016/0370-2693(82)91191-1.
[10] N. Cindro, M. Korolija, D. Shapira, Prog. Part. Nucl. Phys. 30 (1993) 65–73, https://doi.org/10.1016/0146-6410(93)90006-2.
[11] J. Papp, J. Jaros, L. Schroeder, J. Staples, H. Steiner, A. Wagner, J. Wiss, Phys. Rev. Lett. 34 (1975) 601–604, https://doi.org/10.1103/PhysRevLett.34.601.
[12] L.P. Csernai, W. Greiner, H. Stöcker, I. Tanihata, S. Nagamiya, J. Knoll, Phys. Rev. C 25 (1982) 2482–2490, https://doi.org/10.1103/PhysRevC.25.2482.
[13] R.L. Hatch, S.E. Koonin, Phys. Lett. B 81 (1979) 1–4, https://doi.org/10.1016/0370-2693(79)90701-9.
[14] J. Cugnon, Phys. Rev. C 22 (1980) 1885–1896, https://doi.org/10.1103/PhysRevC.22.1885.
[15] I. Tanihata, M.-C. Lemaire, S. Nagamiya, S. Schnetzer, Phys. Lett. B 97 (1980) 363–366, https://doi.org/10.1016/0370-2693(80)90620-6.
[16] S.E. Koonin, Phys. Rev. Lett. 39 (1977) 680–684, https://doi.org/10.1103/PhysRevLett.39.680.
[17] D. Bazin, et al., Phys. Rev. Lett. 102 (2009) 232501, https://doi.org/10.1103/PhysRevLett.102.232501, arXiv:0902.2747.
[18] T. Aumann, C.A. Bertulani, J. Ryckebusch, Phys. Rev. C 88 (2013) 064610, https://doi.org/10.1103/PhysRevC.88.064610, arXiv:1311.6734.
[19] A. Gade, et al., Phys. Rev. C 77 (2008) 044306, https://doi.org/10.1103/PhysRevC.77.044306.
[20] L. Atar, et al., Phys. Rev. Lett. 120 (2018) 052501, https://doi.org/10.1103/PhysRevLett.120.052501.
[21] V.G.J. Stoks, R.A.M. Klomp, M.C.M. Rentmeester, J.J. de Swart, Phys. Rev. C 48 (1993) 792–815, https://doi.org/10.1103/PhysRevC.48.792.
[22] D. Bertini, J. Phys. Conf. Ser. 331 (2011) 032036, https://doi.org/10.1088/1742-6596/331/3/032036.
[23] D. Bertini, M. A-Turany, I. Koenig, F. Uhlig, J. Phys. Conf. Ser. 119 (2008) 032011, https://doi.org/10.1088/1742-6596/119/3/032011.
[24] V. Panin, et al., Phys. Lett. B 753 (2016) 204–210, https://doi.org/10.1016/j.physletb.2015.11.082.
[25] J.M. Kidd, P.J. Lindstrom, H.J. Crawford, G. Woods, Phys. Rev. C 37 (1988) 2613–2623, https://doi.org/10.1103/PhysRevC.37.2613.
[26] W.R. Webber, J.C. Kish, D.A. Schrier, Phys. Rev. C 41 (1990) 547–565, https://doi.org/10.1103/PhysRevC.41.547.
[27] T. Ogawa, T. Sato, S. Hashimoto, D. Satoh, S. Tsuda, K. Niita, Phys. Rev. C 92 (2015) 024614, https://doi.org/10.1103/PhysRevC.92.024614.
[28] B.A. Brown, P.G. Hansen, B.M. Sherrill, J.A. Tostevin, Phys. Rev. C 65 (2002) 061601, https://doi.org/10.1103/PhysRevC.65.061601.
[29] C. Langer, et al., Phys. Rev. C 89 (2014) 035806, https://doi.org/10.1103/PhysRevC.89.035806.
[30] P.J.A. Buttle, Comput. Phys. Commun. 14 (1978) 133–143, https://doi.org/10.1016/0010-4655(78)90056-5.
[31] I.J. Thompson, Comput. Phys. Rep. 7 (1988) 167–212, https://doi.org/10.1016/0167-7977(88)90005-6.
[32] Z. Podolyák, et al., Phys. Rev. Lett. 117 (2016) 222302, https://doi.org/10.1103/PhysRevLett.117.222302.
[33] J. Bystricky, et al., J. Phys. 48 (1987) 1901, https://doi.org/10.1051/jphys:0198700480110190100.